Fabrication and characterization of silicone-based dielectric elastomer actuators for mechanical stimulation of living cells

A. Poulin; S. Rosset; H. Shea

Proceedings Volume 10594, Electroactive Polymer Actuators and Devices (EAPAD) XX; 105940V (2018);

doi: 10.1117/12.2295687

Fabrication and characterization of silicone-based dielectric elastomer actuators for mechanical stimulation of living cells

A. Poulin, S. Rosset and H. Shea
Soft Transducers Laboratory, Ecole Polytechnique Fédérale de Lausanne (EPFL), Neuchâtel, Switzerland

ABSTRACT

Cellular biology is a promising field of application for dielectric elastomer actuators (DEAs) given that large strains are needed but only low forces are required. The development of devices compatible with standard cell culture protocols and equipment is however challenging. We recently demonstrated that DEAs can be interfaced with living cells and used to control their mechanical environment. Here we detail the fabrication process of our DEA-based cell stretcher and present a holder which was designed to provide a simple and safe experience for our biologist partners. We also evaluate the actuation performance of the device in terms of strain amplitude, spatial distribution and stability during periodic actuation. Results show that the device can generate more than 30% uniaxial tensile strain, and achieve more than 12 h of stable actuation performance when cycled between 0% and 12% strain at a 1 Hz frequency.

Keywords: Dielectric elastomer actuators, cell stretcher, strain mapping, reliability

1. INTRODUCTION

It has been demonstrated that mechanical stimulation can affect the growth and development of cells and tissues[1]. While mechanosensitivity has been observed on different cell types[2], the understanding of the mechanisms by which cells can sense their mechanical environment and transduce this information into a biochemical response is still very limited. Due to the complexity of the in vivo environment, studies in this field often rely on in vitro experiments. There is therefore a need for systems that can be used to apply controlled mechanical stimulation on cultured cells. The mechanical stimulation needed for a given experiment can be tensile[3], compressive[4] or shear stress[5]. It can also be applied on different types of cultures such as single cells[6], cell monolayers[7], or 3D cell cultures[8].

Here we are interested in systems which can apply tensile strain on cultured cell monolayers. To generate this type of mechanical stimuli, cells are typically cultured on top of a soft elastomer membrane which is then stretched. With the help of fibronectin or collagen to promote adhesion[9], cells attach to the surface and thus deform together with the membrane. Commercial systems based on this approach are distributed by several companies including Flexcell[10] which uses pneumatic actuation to deform the membrane, and Strex[11] which uses linear motors. While the commercially available systems are a reliable solution, they are often bulky. Their size is an important limitation since it makes it difficult to integrate them with standard equipment for cell culture and imaging. In addition, advances in our understanding of cellular mechanosensitivity would benefit from high-throughput experiments where many different parameters can be varied in parallel. Such experiment are however difficult to implement when working with expensive and bulky equipment.

Miniaturized cell stretchers have been developed to address the limitations of commercially available technologies[12]. Most approaches rely on pneumatic actuation, taking advantage of well-established materials and fabrication processes from the field of microfluidics. In all systems, one or multiple pneumatic chambers are used to deform a suspended elastomer membrane on which cells are cultured. Radial strain can be generated with a chamber located underneath[13] or around[14] a circular membrane. Linear strain can be generated with two chambers located on opposite sides of a square membrane[15]. In this configuration, adding a second set of chambers enables much greater flexibility on the strain profile[16]. While miniaturized pneumatic cell stretcher provide simple and reliable systems, parallelization is not practical due to the need for external pneumatic components. The pumps, valves and tubing quickly become problematic for integrated array of individually addressable elements.

0277-786X/18/$18 · doi: 10.1117/12.2295687

An alternative approach is actuation using Dielectric Elastomer Actuators (DEAs), a method which enables miniaturization[17] and parallelization[18]. We have demonstrated in prior work that DEAs can be interfaced with cell monolayers and used to accurately control the cell's mechanical environment[19]. DEAs are made of an elastomer membrane sandwiched between two stretchable electrodes[20]. When a voltage difference is applied it creates an electrostatic force between the two electrodes that induces thinning of the membrane and surface expansion due to the elastomer incompressibility (Poisson's ratio equal to 0.5). As a proof of concept, we cultured lymphatic endothelial cells on a DEA and stretched them periodically by 10% for 24 h[19]. The cells responded to the mechanical stimulation by aligning perpendicular to the stretch direction, thus demonstrating that DEAs can be used for cell stretching experiments. While our design can provide uniaxial strain, a different DEA configuration for radial strain was also reported[21].

The development of a cell stretcher presents many requirements and challenges. The device has to be biocompatible and sustain and withstand standard cell culture protocols such as sterilization, immersion in conductive cell culture medium, and incubation. Optical transparency is another key parameter as it enables in situ live cell imaging, a capability which can provide insight in the dynamics of cell mechanosensitivity. In terms of mechanical stimulation, the needs greatly vary depending on the cell types and the different stages of cellular response. Whereas cellular sensing mechanisms can occur within seconds, days of mechanical stimulation are often required before gene expression is induced[22]. In practice, in vitro experiment often apply between 5% and 20% strain, at frequencies below 5 Hz, and for durations ranging from 2 hours to 48 hours[1].

We previously demonstrated that DEAs can be interfaced with living cells and used to control their mechanical environment, and that the high voltages used to operate the DEAs had no effect on cell development thanks to careful electrode design[19]. Here we detail the fabrication process of the device and discuss key elements of its design. The ease of operation and safety considerations due to high voltages are important consideration in multidisciplinary projects like this one where non-experts in DEAs (i.e. biologists) will use the device. We therefore developed and present here a holder that makes handling and actuation of the cell stretcher safe and easy. Finally, we also evaluate the actuation performance of the device in terms of strain amplitude, uniformity and stability over periodic actuation. It is very important to know exactly what strain is applied by the cell stretcher to be able to draw strong conclusions from the experiments with cells. Figure 1 (a) presents the fabricated device, its holder, and the high-voltage power supply. The compact system easily fits on a standard microscope as shown in Figure 1 (b). The device working principle is schematized in Figure 1 (c).

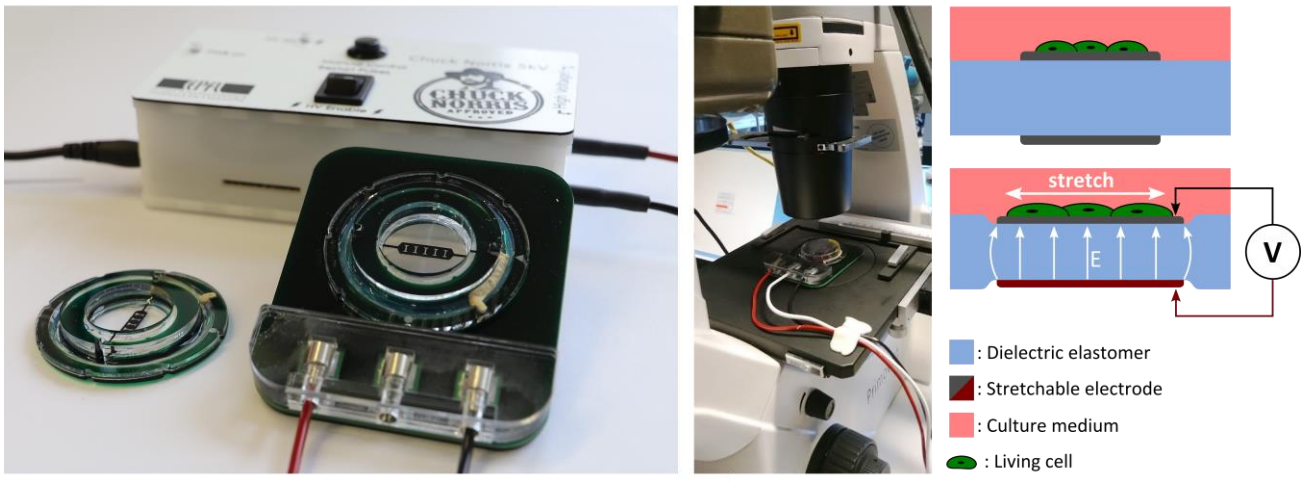

Figure 1: (a) This picture shows a fabricated cell stretcher ready for cell culture on the left hand-side, a device mounted in the holder that connects it to a power supply on the right hand-side, and the high-voltage power supply that drives the actuator in the background. (b) This picture shows the compact system assembled on a microscope and ready for optical inspection of the cultured cells during stretching. (c) Schematic describing the working principle of the cell stretcher. The cells cultured on top of the device deform with the actuator when a voltage difference is applied between the two electrodes. The electrostatic forces generated between the electrodes squeeze the membrane, which then expands in-plane.

0277-786X/18/$18 · doi: 10.1117/12.2295687

2. CELL STRETCHER FABRICATION

The main steps of the cell stretcher fabrication process are presented in Figure 2. For additional information on casting of silicone elastomer membranes, preparation and patterning of carbon-elastomer composite electrodes, and laser manufacturing of PMMA parts for quick prototyping, detailed processes are accessible in a scientific video article[23].

We first stretch a silicone elastomer (Sylgard 186, DowCorning) membrane and assemble it between two rigid PMMA frames using pressure sensitive adhesive (ARclear 8932EE, Adhesive Research) and silicone RTV (Silpuran 4200, Wacker) as presented in Figure 2 (a). The silicone sealant provides a gradual transition between the hard plastic frame and the soft elastomer membrane, a smooth transition that helps avoid stress points which could rupture the thin elastomer film. The membrane thickness indeed decreases from 100 μm to 30 μm after being stretched by λ_H=2.7 and λ_L=1.2. The roles of prestretch are to suppress electromechanical instability in the DEA[24], and provide preferential actuation along λ_L by effectively stiffening the elastomer along λ_H[17].

Stretchable electrodes are then applied on both sides of the membrane to create the DEA as presented in Figure 2 (b). This electrode design provides 5 transparent regions where cells can be stretched and imaged[25]. The top electrode is connected to ground and the bottom electrode is connected to a high-voltage. The electrodes are made of a carbon-elastomer composite which is applied using pad-printing and heat cured at 80°C for 1 hour. The resulting electrodes are approximately 2 μm thick and create a strong chemical bond with the elastomer membrane. They provide good structural stability and can sustain stretching, mechanical abrasion and liquid immersion[26,27]. At this step of the fabrication process it is also possible to print a 3-5 μm thick layer of silicone on top of the device[28]. Covering the electrodes with this passivation layer has several advantages: it decouples the actuator performance and biocompatibility requirements, and provides a more uniform surface for cell culture.

A second set of rigid PMMA frames are fixed on the membrane and create two reservoirs as shown in Figure 2 (c). The top reservoir acts as a cell culture chamber and is designed to contain 1-2 ml of culture medium. The 5 mm thick frame is fixed on the device using a thin layer of biocompatible silicone (Silbione LSR4305, Bluestar Silicones) which is cured at 80°C for 1 hour. The bottom reservoir serves to create an encapsulated oil backing that will cover the backside of the membrane. It is assembled on the device using pressure sensitive adhesive and silicone RTV to avoid pressure points that could rupture the thin membrane. The design ensures that no active region of the DEA is squeezed between two frames which could induce premature dielectric breakdown. The frames are also patterned with openings that give access to the DEA electrodes for electrical contacts.

The DEA is electrically connected using conductive silicone RTV (SS-27S, Silicone Solutions) as presented in Figure 2 (d). The conductive RTV is an elastomer filled with silver particles that provides a more robust contact interface than the pad-printed carbon electrodes. The contact between those silver-based and carbon-based conductors is made over an immobilized region of the membrane, thus avoiding any degradation induced mechanical deformation. The external PMMA frames have a 1 mm wide circular opening which is filled with conductive RTV to connect the top electrode to the bottom side of the device. This step requires puncturing the membrane, which is possible because the silicone RTV ring applied in the first fabrication step stops the propagation of any tear in the membrane. Although the conductive RTV cures at room temperature, we achieved better conductivity and reproducibility by curing it at 80°C for 1 hour.

The final fabrication step is to encapsulate a thin layer of oil on the backside of the membrane as presented in Figure 2 (e). A spacer made of two layers of pressure sensitive silicone adhesive is placed on the backside of the membrane, overlapping with the top PMMA frame which has a slightly smaller inner diameter than the bottom PMMA frame. A glass coverslip is laser etched to create u-shaped inlet and outlet, placed on top of the spacer, and fixed in place using silicone RTV. After curing the device at 80°C for 1 hour, the reservoir is filled with safflower oil, and the inlet and outlet are sealed using silicone RTV. One important role of the oil layer is to isolate the cells from the environment on the other side of the membrane, otherwise only separated by 30 μm of silicone elastomer, an intrinsically permeable material. Another important role is to avoid the creation of superficial cracks that can be observed at the surface of the membrane after a few thousands actuation cycles in air. While those cracks have no impact on the device performance, they affect the optical quality of the system and are therefore undesirable.

The 52 mm-wide and 6 mm-thick final device can be easily manipulated during cell culture, and with less than 300 μm separating the cells from the glass coverslip, standard transmission optical microscopes can be used for in-situ optical inspection. The ground and high-voltage electrodes can both be connected from the bottom side of the device, making the electrical connections easier as explained in the next section.

0277-786X/18/$18 · doi: 10.1117/12.2295687

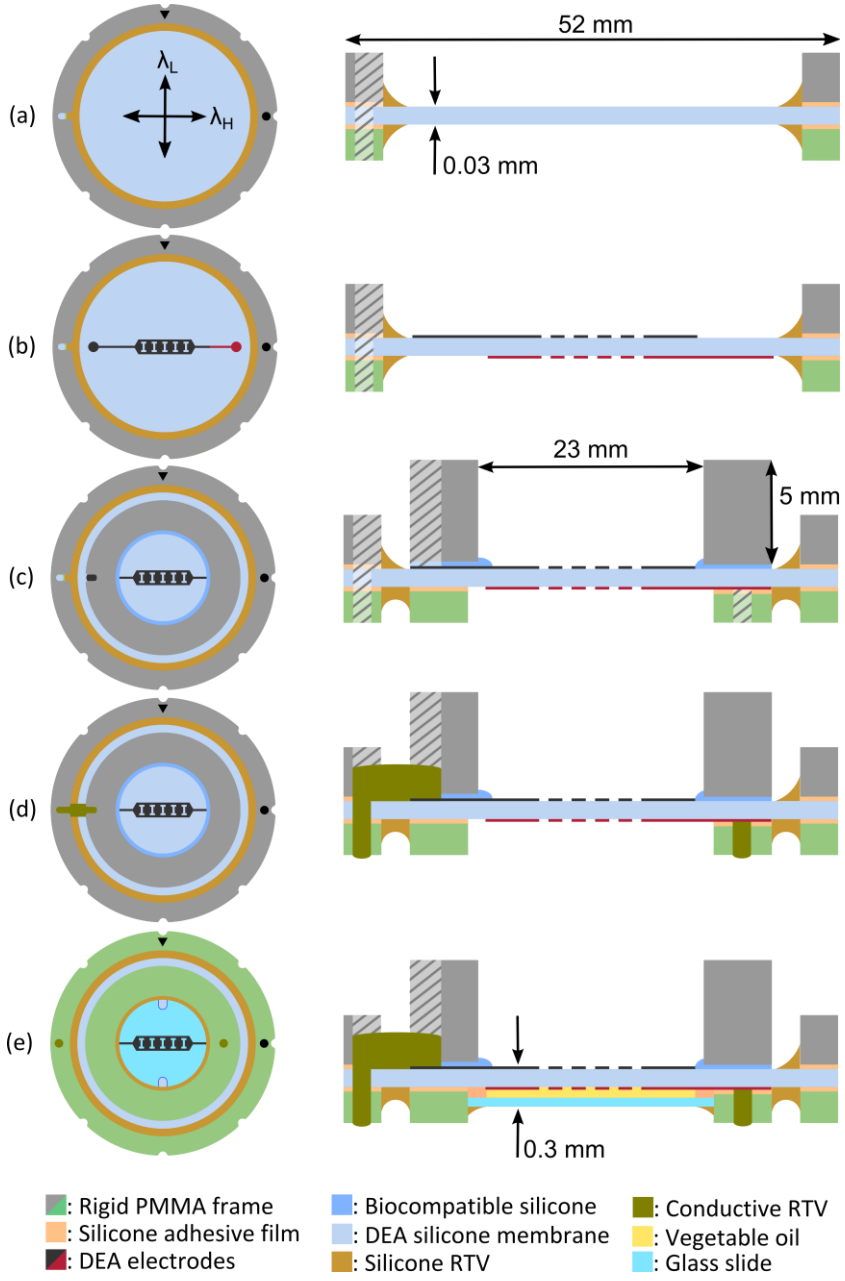

Figure 2: This schematic presents the main fabrication steps of the cell stretcher. (a) The membrane is first stretched and fixed to a rigid PMMA frame using pressure sensitive adhesive and RTV silicone. (b) Carbon-elastomer composite electrodes are patterned on both side of the membrane and create the DEA. (c) Two rigid PMMA frames are added to create reservoirs on both sides of the membrane. The top reservoir is the cell culture chamber, while the bottom reservoir is used to immerse the backside of the membrane in oil. (d) Electrical contacts are made using conductive RTV. After this step, the ground and high-voltage electrodes can be both connected from the bottom side of the device. (e) A plastic spacer and a glass coverslip are assembled on the backside of the membrane to create an oil reservoir which is filled and sealed using silicone RTV.

0277-786X/18/$18 · doi: 10.1117/12.2295687

3. CELL STRETCHER HOLDER FABRICATION

This section presents a holder that connects the cell stretcher to a high-voltage power supply. It was designed to provide a device which is safe and easy to handle. The fabrication process starts with a PMMA plate as presented in Figure 3 (a). The circular opening is there to provide optical access to the culture chamber. The plate is covered by an adhesive layer (ARclear 8932EE, Adhesive Research) on which a PCB is fixed as presented in Figure 3 (b). The PCB has two square contact pads, each connected to a circular contact pad via buried traces. The ground and high-voltage electrodes are shown in black and red respectively. Magnetic connectors are fabricated by soldering brass terminals on the square pads and press-fitting nickel-coated magnets in their cylindrical opening. A PMMA plate with an opening that matches the outer dimension of the cell stretcher is then fixed on top of the PCB as presented in Figure 3 (c). The keyed plate design ensures that the device only fits when its electrical contacts are aligned with the contact pads of the PCB. The last fabrication step is to enclose the magnetic connectors as presented in Figure 3 (e)-(f). The PMMA enclosure is fixed using dichloromethane and has two circular openings located on the front side of the holder, thus giving access to the recessed magnetic connectors.

Connecting the cell stretcher using this holder requires very little manipulation as shown in Figure 3 (g)-(h). A drop of electrolyte conductive gel (Signa gel, Parker) is first dispensed on each circular electrode to ensure good electrical contact, after what the device is simply placed on the holder. The holder is then connected to a high-voltage power supply[29] using custom made wires compatible with the magnetic connectors. The holder is designed to ensure that no high-voltage contacts are exposed once assembled with the device. The compact system can then be safely manipulated and installed on a microscope or in a culture incubator for an experiment.

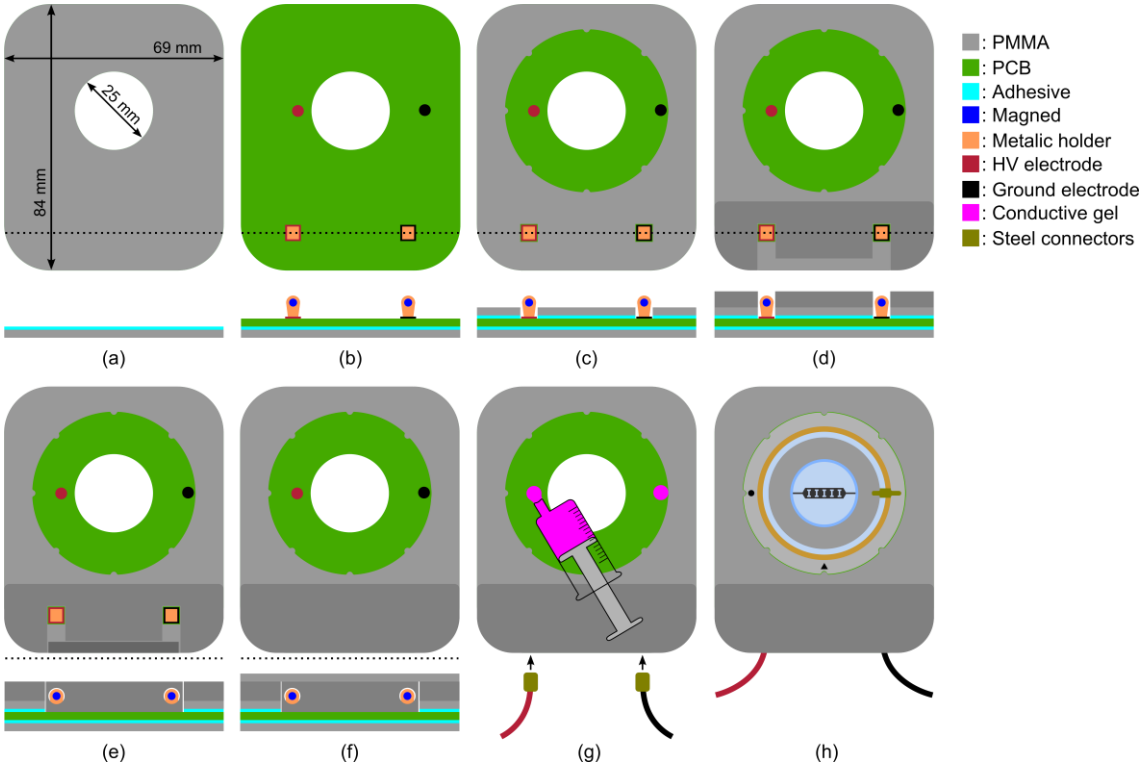

Figure 3: Schematic diagrams showing top and cross-section views of the holder through its main fabrication steps. (a) The fabrication starts with a PMMA plate covered on one side with adhesive and with a circular opening that matches the size of the cell stretcher culture chamber. (b) The adhesive is used to fix a PCB which has two square contacts, each connected via buried traces to a circular contact. Brass connectors are soldered on the square contacts, and nickel-coated magnets are press-fitted in the cylindrical opening of the connectors. (c) A PMMA plate with an opening that matches the outer dimension of the cell stretcher is fixed on top of the PCB using adhesive. (d)-(f) The exposed brass connectors are enclosed with PMMA parts fixed in place using dichloromethane, leaving only two circular opening in front of the holder. (g)-(h) The cell stretcher is connected by simply dispensing a drop of electrolyte conductive gel on each circular electrode and positioning the device on top. A high-voltage power supply is connected to the holder using custom made steel connectors.

4. ACTUATION STRAIN AMPLITUDE, UNIFORMITY AND STABILITY

The actuation performance of the device was characterized in terms of strain amplitude, uniformity and stability. The cell culture conditions were reproduced by filling the top reservoir with growth medium (and the back reservoir with safflower oil) during the measurements. Growth medium is a conductive aqueous solution and its presence can affect the DEA performance by acting as a blanket electrode[30]. Its presence can also lead to the diffusion of ions in the membrane and induce premature dielectric breakdown. It is therefore important to take the growth medium into consideration when characterizing the actuation performance.

The measured strain-voltage response is presented in Figure 4 (a) and shows a maximum strain of $\varepsilon_{\lambda L}$=30.6% at a driving voltage of 4.7 kV. The deformation generated along the low stretch orientation λ_L is accompanied by a significantly smaller deformation along the high stretch orientation λ_H, equal to $\varepsilon_{\lambda H}$=5.6% at a driving voltage of 4.7 KV. This large anisotropy is caused by the non-equibiaxial stretch that was applied on the membrane during fabrication. The maximum strain is limited by loss of mechanical tension and not by dielectric breakdown or electromechanical instability. Higher strain could be achieved by increasing the membrane prestretch along λ_L. It would however stiffen the membrane and therefore increase the driving electric field, and most importantly decrease the ratio $\varepsilon_{\lambda L}/\varepsilon_{\lambda H}$. In addition, a linear tensile strain of 30% is already enough when compared with biologically relevant strain levels and commercially available cell stretching systems.

The actuation strain $\varepsilon_{\lambda L}=1-e_a/e_r$ was obtained from the width of the electrodes measured at rest e_r and in the actuated state e_a. Similarly, the actuation strain $\varepsilon_{\lambda H}=1-g_a/g_r$ was obtained from the width of the electrodes gap measured at rest g_r and in the actuated state g_a. While this strain measurement method is reliable and easy to implement, it only gives the average strain in the electrode gap and provides no information on the uniformity of the strain profile. To obtain a strain map, we used a digital image correlation tool[31] and processed pictures of the actuator at rest and in the actuated state. Figure 4 (b) presents the strain profile we obtained using this technique. The results show a uniform strain distribution in the center of the electrode gap, while boundary effects are visible at its edges. The strain profile is strongly affected by the aspect ratio e/g which should be maximised for better uniformity. For this specific device the gap was e=2.5 mm large by g=1 mm wide.

We also characterized the cell stretcher stability over cyclic actuation. The device was actuated using a National Instrument Data Acquisition module connected to a high-voltage power amplifier (609E-6, Trek), and imaged using a USB camera mounted on an optical microscope. The setup was controlled via LabVIEW and used to cycle the device between 0 V and 4 kV with a 1 Hz square wave function. The strain was measured at 0 V and 4 kV after every 1'000 actuation cycles, whereas a full strain-voltage curve was measured after every 10'000 cycles. The driving voltage was applied and kept constant for 1 s before each strain measurement. Figure 5 (a) shows the evolution of the strain as a function of the number of actuation cycles. A drift of the strain-voltage curve can be observed between cycles 1 and 10'000, but it then remains stable over the next 70'000 cycles. The experiment was stopped after more than 22 hours or 80'000 actuation cycles due to a failure of the DEA by dielectric breakdown.

To help visualizing the evolution of the cell stretcher response, results from Figure 5 (a) can be projected on the strain-cycles plane as shown in Figure 5 (b). In addition, the number of cycles was converted to actuation time using the frequency of the driving signal, and only 5 measurement points from the strain-voltage curves were kept. The results show a remaining strain of approximately 1.5% when de device is at rest. This effect can be due to a combination of stress relaxation, viscoelasticity, and plastic deformation of the membrane and the electrodes. It is interesting to note that the strain also increases in the actuated state, and that the amplitude of the drift increases with the driving voltage. The processes leading to the change of the strain-voltage response are complex. The objective of this work is not to identify these processes, but to quantify their impact on the stability of the device over cyclic actuation. We repeatedly observed that the response of the cell stretcher quickly drifts by 1-2% strain over cyclic actuation, after which it exhibits very stable actuation performance.

0277-786X/18/$18 · doi: 10.1117/12.2295687

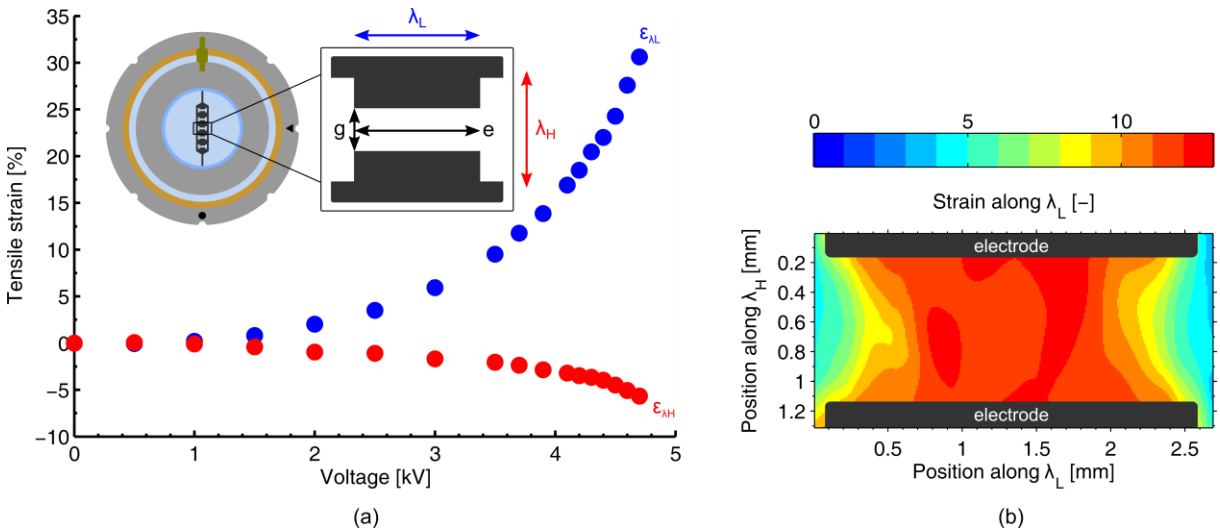

Figure 4: (a) This graph presents the strain-voltage response of the device, showing more than 30% tensile strain at 4.7 kV. The strain $\varepsilon_{\lambda L}$ in the low stretch orientation λ_L was measured by tracking the distance e between edges of the DEA electrodes. The strain $\varepsilon_{\lambda H}$ in the high stretch orientation λ_H was measured by tracking the distance g between the edges of the DEA electrodes. (b) This image presents the measured strain profile of the cell stretcher, showing good uniformity in the center of the electrode gap where cells are cultured and stretched. The strain was measured by processing pictures of the actuator at rest and actuated using digital image correlation.

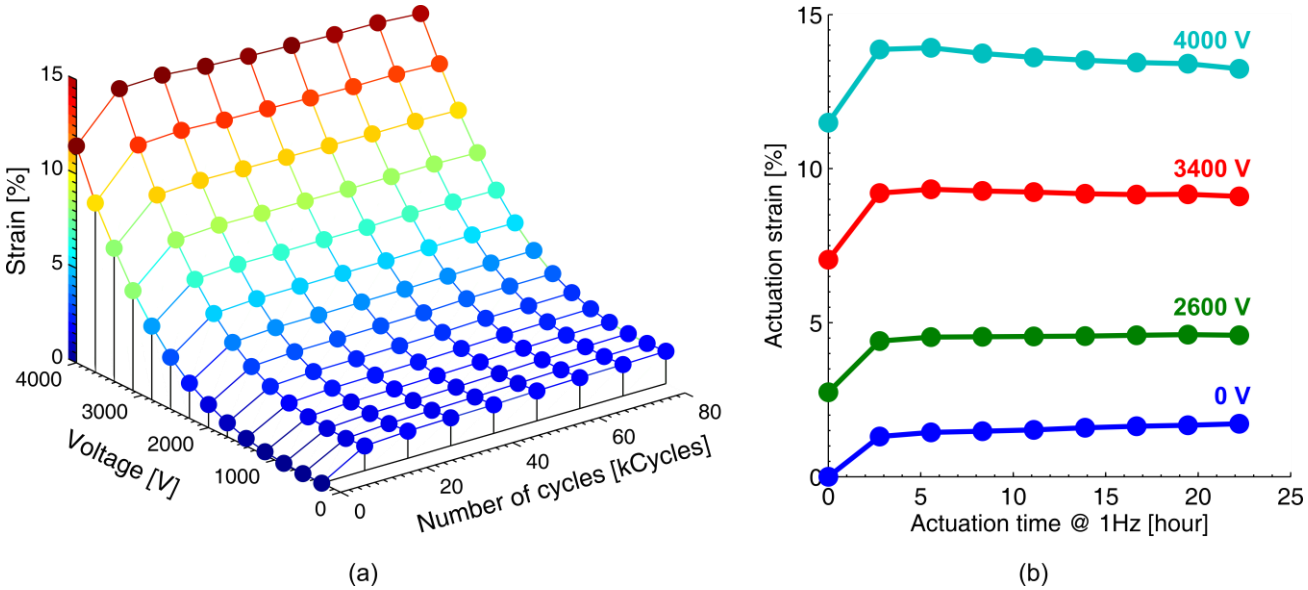

Figure 5: (a) This graph presents voltage-strain curves of the device which were measured every 10’000 cycles during a cyclic actuation at 1 Hz. (b) This graph presents a projection of the data from the graph on the left. It shows the evolution of the actuation strain at four different voltages over more than 20 hours of cyclic actuation at 1 Hz. After an initial drift of the strain-voltage response by approximately 1.5% strain, the device shows stable operation for more than 20 hours of cyclic actuation.

5. CONCLUSION

In this work, we presented a reliable fabrication process for DEA-based deformable cell stretchers. With its silicone membrane and carbon-elastomer composite electrodes, the device provides a biocompatible environment which is also compatible with standard cell culture protocols such as sterilization and immersion in growth medium. A high fabrication yield was achieved by optimizing the adhesion of the highly pre-stretched membrane to its support frames. The use of RTV silicone as a soft transition between the hard frames and the soft membrane was a key element in avoiding local pressure points that would otherwise puncture the membrane. The encapsulation of an oil layer below the actuator suppressed the growth of superficial cracks over long periods of cyclic actuation.

We also presented the development of a holder adapted to working in multidisciplinary projects where partners are not necessarily experts in DEAs. The holder is designed to make handling and connection of the DEA simple and safe. Connecting the device only requires dispensing a drop of electrolyte conductive gel on each electrode and placing the device on the holder. The holder is then connected to a high-voltage power supply with magnetic connectors which enable quick and easy connection. The system is designed to ensure that there are not exposed high-voltage contacts once the sample is assembled and the high-voltage power supply is connected.

The actuation performance of the cell stretcher was evaluated in terms of strain amplitude, uniformity and stability. The device demonstrated more than 30% uniaxial tensile strain and showed good strain uniformity. The device stain-voltage response was measured over periodic actuation and showed good stability over more than 80’000 cycles. The duration of the experiments was limited by dielectric breakdown of the DEA. While the device lifetime already enables many interesting mechanobiology experiments, it could be improved to provide a more universal platform for cell stretching experiments.

ACKNOWLEDGEMENTS

This work was supported by the Swiss National Science Foundation (SNSF) under the grants No. CR32I3_166326 and 200020_165993.

REFERENCES

[1] Wang, J. H.-C.., Thampatty, B. P., “An Introductory Review of Cell Mechanobiology,” Biomech. Model. Mechanobiol. **5**(1), 1–16 (2006).

[2] Giulitti, S., Zambon, A., Michielin, F.., Elvassore, N., “Mechanotransduction through substrates engineering and microfluidic devices,” Curr. Opin. Chem. Eng. **11**, 67–76, Elsevier Ltd (2016).

[3] Bleuel, J., Zaucke, F., Brüggemann, G.-P.., Niehoff, A., “Effects of Cyclic Tensile Strain on Chondrocyte Metabolism: A Systematic Review,” PLoS One **10**(3), M. Lammi, Ed., e0119816 (2015).

[4] Rosa, N., Simoes, R., Magalhães, F. D.., Marques, A. T., “From mechanical stimulus to bone formation: A review,” Med. Eng. Phys. **37**(8), 719–728 (2015).

[5] Sabine, A., Agalarov, Y., Maby-El Hajjami, H., Jaquet, M., Hägerling, R., Pollmann, C., Bebber, D., Pfenniger, A., Miura, N., et al., “Mechanotransduction, PROX1, and FOXC2 Cooperate to Control Connexin37 and Calcineurin during Lymphatic-Valve Formation,” Dev. Cell **22**(2), 430–445 (2012).

[6] Scuor, N., Gallina, P., Panchawagh, H. V., Mahajan, R. L., Sbaizero, O.., Sergo, V., “Design of a novel MEMS platform for the biaxial stimulation of living cells,” Biomed. Microdevices **8**(3), 239–246 (2006).

[7] Kamotani, Y., Bersano-Begey, T., Kato, N., Tung, Y.-C., Huh, D., Song, J. W.., Takayama, S., “Individually programmable cell stretching microwell arrays actuated by a Braille display,” Biomaterials **29**(17), 2646–2655 (2008).

[8] Moraes, C., Wang, G., Sun, Y.., Simmons, C. a., “A microfabricated platform for high-throughput unconfined compression of micropatterned biomaterial arrays,” Biomaterials **31**(3), 577–584, Elsevier Ltd (2010).

[9] Khalili, A.., Ahmad, M., “A Review of Cell Adhesion Studies for Biomedical and Biological Applications,” Int.

0277-786X/18/$18 · doi: 10.1117/12.2295687

J. Mol. Sci. **16**(12), 18149–18184 (2015).

[10] "Flexcell International Corporation.", <http://www.flexcellint.com/> (25 August 2016).

[11] "Strex USA.", <https://strexcell.com> (25 September 2016).

[12] Kim, D.-H., Wong, P. K., Park, J., Levchenko, A.., Sun, Y., "Microengineered Platforms for Cell Mechanobiology," Annu. Rev. Biomed. Eng. **11**(1), 203–233 (2009).

[13] Simmons, C. S., Sim, J. Y., Baechtold, P., Gonzalez, A., Chung, C., Borghi, N.., Pruitt, B. L., "Integrated strain array for cellular mechanobiology studies," J. Micromechanics Microengineering **21**(5), 54016 (2011).

[14] Kreutzer, J., Ikonen, L., Hirvonen, J., Pekkanen-Mattila, M., Aalto-Setälä, K.., Kallio, P., "Pneumatic cell stretching system for cardiac differentiation and culture," Med. Eng. Phys. **36**(4), 496–501, Institute of Physics and Engineering in Medicine (2014).

[15] Huang, Y.., Nguyen, N.-T., "A polymeric cell stretching device for real-time imaging with optical microscopy," Biomed. Microdevices **15**(6), 1043–1054 (2013).

[16] Tremblay, D., Chagnon-Lessard, S., Mirzaei, M., Pelling, A. E.., Godin, M., "A microscale anisotropic biaxial cell stretching device for applications in mechanobiology," Biotechnol. Lett. **36**(3), 657–665 (2014).

[17] Akbari, S.., Shea, H. R., "An array of 100μm×100μm dielectric elastomer actuators with 80% strain for tissue engineering applications," Sensors Actuators A Phys. **186**, 236–241 (2012).

[18] Marette, A., Poulin, A., Besse, N., Rosset, S., Briand, D.., Shea, H., "Flexible Zinc-Tin Oxide Thin Film Transistors Operating at 1 kV for Integrated Switching of Dielectric Elastomer Actuators Arrays," Adv. Mater. **29**(30), 1700880 (2017).

[19] Poulin, A., Saygili Demir, C., Rosset, S., Petrova, T. V.., Shea, H., "Dielectric elastomer actuator for mechanical loading of 2D cell cultures," Lab Chip **16**(19), 3788–3794, Royal Society of Chemistry (2016).

[20] Pelrine, R., Kornbluh, R., Pei, Q.., Joseph, J., "High-Speed Electrically Actuated Elastomers with Strain Greater Than 100%," Science. **287**, 836–839 (2000).

[21] Cei, D., Costa, J., Gori, G., Frediani, G., Domenici, C., Carpi, F.., Ahluwalia, A., "A bioreactor with an electro-responsive elastomeric membrane for mimicking intestinal peristalsis," Bioinspir. Biomim. **12**(1), 16001, IOP Publishing (2016).

[22] Iskratsch, T., Wolfenson, H.., Sheetz, M. P., "Appreciating force and shape — the rise of mechanotransduction in cell biology," Nat. Rev. Mol. Cell Biol. **15**(12), 825–833, Nature Publishing Group (2014).

[23] Rosset, S., Araromi, O. A., Schlatter, S.., Shea, H. R., "Fabrication Process of Silicone-based Dielectric Elastomer Actuators," J. Vis. Exp. **108**(108), 231–238 (2016).

[24] Koh, S. J. A., Li, T., Zhou, J., Zhao, X., Hong, W., Zhu, J.., Suo, Z., "Mechanisms of large actuation strain in dielectric elastomers," J. Polym. Sci. Part B Polym. Phys. **49**(7), 504–515 (2011).

[25] Rosset, S., Poulin, A., Zollinger, A., Smith, M.., Shea, H., "Dielectric elastomer actuator for the measurement of cell traction forces with sub-cellular resolution," Proc. SPIE 10163, Electroact. Polym. Actuators Devices, Y. Bar-Cohen, Ed., 101630P (2017).

[26] de Saint-Aubin, C. A., Rosset, S., Schlatter, S.., Shea, H., "High-cycle electromechanical aging of dielectric elastomer actuators with carbon-based electrodes," Smart Mater. Struct. **15**(1), 13001 (2017).

[27] Rosset, S., de Saint-Aubin, C., Poulin, A.., Shea, H. R., "Assessing the degradation of compliant electrodes for soft actuators," Rev. Sci. Instrum. **88**(10), 105002 (2017).

[28] Poulin, A., Rosset, S.., Shea, H. R., "Printing low-voltage dielectric elastomer actuators," Appl. Phys. Lett. **107**(24), 244104 (2015).

[29] Rosset, S., Schlatter, S.., Shea, H., "Project Peta-pico-Voltron," <http://petapicovoltron.com/> (5 February 2017).

[30] Poulin, A., Maffli, L., Rosset, S.., Shea, H., "Interfacing dielectric elastomer actuators with liquids," Proc. SPIE 9430, Electroact. Polym. Actuators Devices, Y. Bar-Cohen, Ed., 943011, San Diego (2015).

[31] Blaber, J., "Ncorr," 1.2.

0277-786X/18/$18 · doi: 10.1117/12.2295687